0090-9556/10/3803-431–440$20.00
DRUG METABOLISM AND DISPOSITION
Vol. 38, No. 3
28712/3560030
Printed in U.S.A.

DMD 38:431–440, 2010

Glucuronidation of Dihydrotestosterone and *trans*-Androsterone by Recombinant UDP-Glucuronosyltransferase (UGT) 1A4: Evidence for Multiple UGT1A4 Aglycone Binding Sites

Jin Zhou, Timothy S. Tracy, and Rory P. Remmel

Departments of Medicinal Chemistry (J.Z., R.P.R.) and Experimental and Clinical Pharmacology (T.S.T.), University of Minnesota, Minneapolis, Minnesota

Received June 12, 2009; accepted December 3, 2009

ABSTRACT:

UDP-glucuronosyltransferase (UGT) 1A4-catalyzed glucuronidation is an important drug elimination pathway. Although atypical kinetic profiles (nonhyperbolic, non-Michaelis-Menten) of UGT1A4-catalyzed glucuronidation have been reported occasionally, systematic kinetic studies to explore the existence of multiple aglycone binding sites in UGT1A4 have not been conducted. To this end, two positional isomers, dihydrotestosterone (DHT) and *trans*-androsterone (*t*-AND), were used as probe substrates, and their glucuronidation kinetics with HEK293-expressed UGT1A4 were evaluated both alone and in the presence of a UGT1A4 substrate [tamoxifen (TAM) or lamotrigine (LTG)]. Coincubation with TAM, a high-affinity UGT1A4 substrate, resulted in a concentration-dependent activation/inhibition effect on DHT and *t*-AND glucuronidation, whereas LTG, a low-affinity UGT1A4 substrate, noncompetitively inhibited both processes. The glucuronidation kinetics of TAM were then evaluated both alone and in the presence of different concentrations of DHT or *t*-AND. TAM displayed substrate inhibition kinetics, suggesting that TAM may have two binding sites in UGT1A4. However, the substrate inhibition kinetic profile of TAM became more hyperbolic as the DHT or *t*-AND concentration was increased. Various two-site kinetic models adequately explained the interactions between TAM and DHT or TAM and *t*-AND. In addition, the effect of TAM on LTG glucuronidation was evaluated. In contrast to the mixed effect of TAM on DHT and *t*-AND glucuronidation, TAM inhibited LTG glucuronidation. Our results suggest that multiple aglycone binding sites exist within UGT1A4, which may result in atypical kinetics (both homotropic and heterotropic) in a substrate-dependent fashion.

Glucuronidation, catalyzed by UDP-glucuronosyltransferases (UGTs), is an important elimination pathway of various endogenous compounds such as steroid hormones, bile acids, and bilirubin, as well as a large number of xenobiotics including drugs and their metabolites (Tukey and Strassburg, 2000). Of the 21 functional human UGT isoforms that have been characterized to date (Mackenzie et al., 2008), human UGT1A4 is often considered as the primary catalyst for *N*-glucuronidation because of its efficiency in catalyzing the glucuronidation of primary, secondary, tertiary, and aromatic amines (Kiang et al., 2005). In addition to different amines, steroidal compounds with hydroxyl groups such as diosgenin and hecogenin are also UGT1A4 substrates (Green and Tephly, 1996).

Human UGTs are integral membrane proteins, with the majority of the protein, including the substrate binding sites (both aglycone and UDPGA), on the luminal side of the endoplasmic reticulum membrane (Radominska-Pandya et al., 1999). Although an apo crystal structure of the cofactor UDP-glucuronic acid (UDPGA) binding domain of human UGT2B7 has recently been published (Miley et al., 2007), the three-dimensional structures of the aglycone binding sites of UGTs are unknown, and the interactions between their aglycone substrates and the substrate binding sites are poorly understood.

Similar to the cytochromes P450 such as CYP3A4, some UGT isoforms also exhibit atypical (non-Michaelis-Menten) kinetic features (Fisher et al., 2000; Uchaipichat et al., 2004; Iwuchukwu and Nagar, 2008; Ohno et al., 2008). Although the molecular mechanism(s) of atypical kinetics is still not fully established, numerous studies with the cytochromes P450 support the hypothesis that simultaneous binding of multiple molecules to the enzyme is involved (Shou et al., 1994; Korzekwa et al., 1998; Kenworthy et al., 2001; Shou et al., 2001; Galetin et al., 2002). Such detailed studies with UGTs are less prevalent. Uchaipichat et al. (2008) recently examined 4-methylumbelliferone, 1-naphthol, and zidovudine glucuronidation by UGT2B7. These authors concluded that the kinetic data provided evidence for the existence of multiple aglycone binding sites in UGT2B7. Rios and Tephly (2002) also proposed that two or more aglycone binding sites may exist within UGT1A1, based on evaluations of the interactions of UGT1A1-catalyzed buprenorphine and bilirubin glucuronidation.

Atypical kinetics of UGT1A4-catalyzed glucuronidation have also been reported (Chouinard et al., 2006; Hashizume et al., 2008; Hyland et al., 2009). However, systematic kinetic studies to explore the

This work was supported in part by the National Institutes of Health National Institute of General Medical Sciences [Grant GM063215] (to T.S.T.); Bristol-Myers Squibb (to R.P.R.); and a grant from Shimadzu was awarded for the purchase of the Shimadzu LCMS-2010A instrument used in this study.

Article, publication date, and citation information can be found at http://dmd.aspetjournals.org.

doi:10.1124/dmd.109.028712.

ABBREVIATIONS: UGT, UDP glucuronosyltransferase; UDPGA, UDP-glucuronic acid; DHT, dihydrotestosterone; *t*-AND, *trans*-androsterone, epiandrosterone; TAM, tamoxifen; LTG, lamotrigine; HPLC, high-performance liquid chromatography; ESI, electrospray ionization; MS, mass spectrometry; DMSO, dimethyl sulfoxide; LC, liquid chromatography; RF, radiofrequency; AICc, second-order Akaike information criterion.

existence of multiple aglycone binding sites in UGT1A4 have never been conducted. Dihydrotestosterone (DHT) and *trans*-androsterone (*t*-AND) (Fig. 1) are two steroidal substrates of UGT1A4. Although the glucuronidation of DHT and *t*-AND by UGT1A4 has been clearly established (Green and Tephly, 1996), a detailed kinetic analysis of these processes has not been reported. These two compounds, based on a planar, rigid steroidal scaffold, differ only with respect to the position of the hydroxyl group (at position 3 or 17, the site of glucuronidation) and the location of the ketone group (position 17 or 3). Because of the rigid steroidal scaffold shared by these two compounds and the differing placement of substituents, these two compounds may either occupy the same region of the active site but in opposite orientation or occupy two separate regions in the UGT1A4 active site. Studies in our laboratory on the activities of two polymorphic UGT1A4 enzymes (UGT1A4.2 and UGT1A4.3) demonstrated that mutations of amino acids in exon 1 of UGT1A4 exhibited a differential effect on DHT and *t*-AND glucuronidation (J. Zhou, T. S. Tracy, and R. P. Remmel, unpublished data). Because it is generally accepted that aglycone substrate binding sites of UGT1A enzymes are within the exon 1-coded N-terminal ends of the proteins (Radominska-Pandya et al., 1999), such polymorphic effects may indicate the possibility of DHT and *t*-AND occupying two separate regions in UGT1A4, reinforcing the need to conduct systematic kinetic studies with these two compounds to explore the existence of multiple aglycone binding sites in UGT1A4. To this end, a detailed characterization of the glucuronidation kinetics of these two compounds by HEK293-expressed UGT1A4 was conducted. Interactions of DHT or *t*-AND with another UGT1A4 substrate [tamoxifen (TAM) or lamotrigine (LTG); structures shown in Fig. 1] were also evaluated.

Materials and Methods

Materials. Tamoxifen citrate and tamoxifen were purchased from MP Biomedicals LLC (Santa Ana, CA). Lamotrigine was purchased from Toronto Research Chemicals Inc. (North York, ON, Canada). Dihydrotestosterone, dihydrotestosterone glucuronide, *trans*-androsterone (epiandrosterone), *trans*-androsterone glucuronide, and testosterone glucuronide were purchased from Steraloids (Newport, RI). Lamotrigine-N_2-glucuronide was a gift from GlaxoSmithKline (Philadelphia, PA). UDPGA, Trizma base, Trizma HCl, D-saccharic acid 1,4-lactone, alamethicin, morphine-3-glucuronide, and aceto-bromo-α-D-glucuronic acid methyl ester were purchased from Sigma-Aldrich (St. Louis, MO). $MgCl_2$ was purchased from Mallinckrodt (Hazelwood, MO). All other chemicals used in the glucuronidation incubations, as well as the HPLC solvents were of HPLC grade. Chemicals used in the synthesis of tamoxifen-*N*-glucuronide were ACS grade. Recombinant UGT1A4 was produced in HEK293 cells (gift from Dr. Philip Lazarus, Penn State University, Hershey, PA). Cell lysate, prepared by sonication of UGT1A4-HEK293 cells in 10 mM Tris buffer (pH 7.4 at 37°C) containing 0.25 M sucrose for three 30-s bursts, each separated by a 1-min cooling on ice, was added directly to the incubation as the enzyme source. The protein concentration in cell lysate was determined with the Pierce BCA protein assay kit (Thermo Fisher Scientific, Waltham, MA).

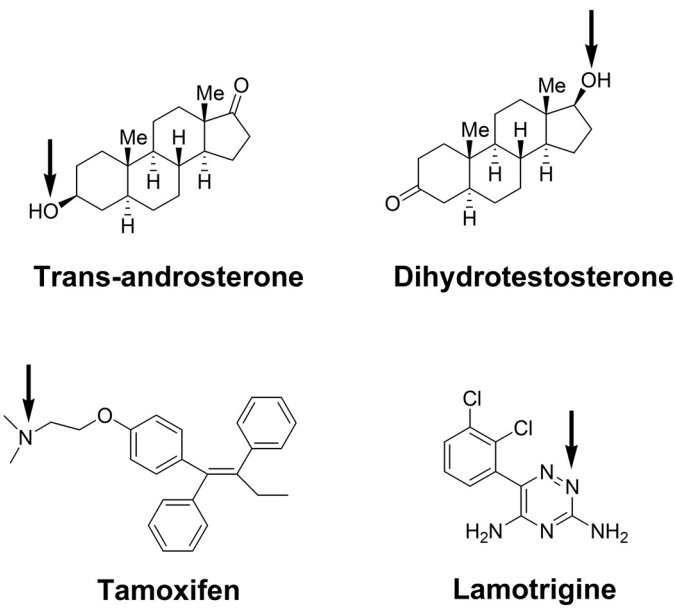

FIG. 1. Structures of DHT, *t*-AND, TAM, and LTG. The glucuronidation sites of the compounds are illustrated with arrows.

Synthesis of Tamoxifen-*N*-glucuronide. Tamoxifen-*N*-glucuronide was synthesized according to the method of Kaku et al., 2004. Fifty milligrams (0.134 mmol) of tamoxifen and 80.2 mg (0.202 mmol) of acetobromo-α-D-glucuronic acid methyl ester were dissolved in 0.4 ml of anhydrous dichloromethane and stirred for 72 h at room temperature under nitrogen protection. The organic solvent was then removed by rotary evaporation. The resulting residue was dissolved in 3 ml of methanol, and 1.5 ml of 0.5 M aqueous sodium carbonate was added to the methanolic solution. The resulting solution was stirred at room temperature for 5 h, and 25 ml of water was then added to the reaction mixture, which was extracted five times with equal volumes of ether to remove unreacted tamoxifen. The pH of the aqueous layer was adjusted to 5.0 with 1 M HCl. Water in the aqueous layer was then removed by lyophilization. The resulting residue was redissolved with a small volume of 0.1% formic acid in MeOH and loaded onto a preparative HPLC column (Haisil HL C18 5 μm, 100 × 20 mm; Higgins Analytical Inc., Mountain View, CA). The tamoxifen glucuronide was eluted with a mobile phase, consisting of 0.1% formic acid in water-0.1% formic acid in MeOH (4:6, v/v), at a flow rate of 22 ml/min and monitored by UV absorbance at 254 nm. The tamoxifen-*N*-glucuronide eluted at 16.5 min, and collected fractions were pooled. Evaporation of the combined eluate fractions yielded 9.8 mg of white powder (13.2%). ^{1}H NMR (600 MHz, dimethyl sulfoxide-d_6): δ 0.885 (t, 3H, J = 7.2 Hz, CH_2CH_3), 2.409 (q, 2H, J = 7.2 Hz, CH_2CH_3), 3.159–3.229 [m, 7H, N–$(CH_3)_2$ and H-4′], 3.329 (m, 1H, H-3′), 3.464 (d, 1H, J = 8.4 Hz, H-5′), 3.589 (m, 1H, H-2′), 3.843–3.886 (m, 2H, N–CH_2CH_2–O), 4.391 (m, 2H, N–CH_2CH_2–O), 4.694 (d, 1H, J = 7.2 Hz, H-1′),6.716 (d, 2H, J 8.4 Hz, ArH, *ortho* to NCH_2CH_2O–), 6.80 (d, 2H, J = 9 Hz, ArH, *meta* to NCH_2CH_2O–), 7.157–7.433 (m, 10H, ArH). ESI-time of flight-MS: 548.2649 $[M]^+$ (error 0.18 ppm).

Incubations to Characterize Glucuronidation Kinetics in the Absence of Modifiers. Preliminary experiments were conducted to ensure that all kinetic determinations were performed under linear conditions with respect to time and protein concentration. Incubation mixtures (200 μl final volume) contained UGT1A4-HEK293 cell lysate (0.25 mg/ml protein for *t*-AND, DHT, and LTG glucuronidation or 0.1 mg/ml protein for TAM glucuronidation), Tris-HCl buffer (0.1 M), $MgCl_2$ (5 mM), D-saccharic acid 1,4-lactone (5 mM), UDPGA (3 mM), alamethicin (50 μg/mg protein), and DHT (3.9–250.0 μM), *t*-AND (2.8–202.2 μM), TAM (0.5–100 μM), or LTG (47.4–4969.8 μM). DHT, *t*-AND, and TAM were initially dissolved in DMSO before addition to the incubation mixtures, whereas LTG was initially dissolved in 0.1 M acetic acid containing 4% DMSO. The final organic solvent concentrations in all incubation mixtures were always ≤2%. In each experiment, the organic concentration was constant irrespective of substrate concentration. The final pH of all incubation mixtures was 7.4 at 37°C. Cell lysates were preincubated on ice with alamethicin for 30 min before reaction initiation. This step was followed by a 3-min preincubation at 37°C, after which the reaction was initiated by addition of UDPGA. After a 30-min (DHT, *t*-AND, and LTG) or 20-min (TAM) incubation in a shaking water bath, reactions were terminated by addition of 200 μl of cold acetonitrile, followed by addition of internal standards (DHT and *t*-AND glucuronidation assay: 20 μl of 1.07 μg/ml testosterone glucuronide; TAM glucuronidation assay: 10 μl of 14.2 μg/ml lamotrigine glucuronide; LTG glucuronidation assay: 10 μl of 50 μg/ml morphine-3-glucuronide). Protein precipitate was removed by centrifugation at 13,000*g* for 5 min, and the reaction mixture was filtered through a 0.2-μm nylon spin filter (Grace Davison Discovery Science, Deerfield, IL) before injection onto the HPLC system.

Incubations to Characterize Interactions between UGT1A4 Substrates. The effect of TAM on DHT and *t*-AND glucuronidation was initially evaluated

with three DHT or *t*-AND concentrations (approximately 0.5 K_m, K_m, and 2 K_m) and six TAM concentrations (0, 1.25, 2.5, 5, 10, and 20 μM). Because we observed a significant activation effect of TAM on DHT glucuronidation in this initial study, the effect of TAM on DHT glucuronidation was further evaluated with seven DHT concentrations (2.5–100 μM) in the absence or presence of five TAM concentrations (2.5–40 μM). The effect of LTG on DHT and *t*-AND glucuronidation was also evaluated with three DHT or *t*-AND concentrations (approximately 0.5 K_m, K_m, and 2 K_m) and six LTG concentrations (0, 0.375, 0.75, 1.5, 3, and 4.5 mM), and the effect of TAM on LTG glucuronidation was studied with three LTG concentrations (0.75, 1.5, and 3 mM) and six TAM concentrations (0, 1.25, 2.5, 5, 10, and 20 μM). The incubation conditions were as described above. To quantify dihydrotestosterone glucuronide by LC-MS, a liquid-liquid procedure was applied after reaction termination and protein precipitation. Fifty microliters of 2.4 mol/l HCl solution were added to the incubation supernatants, and the sample was extracted twice with 500 μl of ethyl acetate. The ethyl acetate extracts were then combined and dried under N_2 gas. Residues were reconstituted with 50 μl of water-acetonitrile (3:7, v/v) and 25 μl of the sample were injected onto the HPLC system for quantification. The recovery of the liquid-liquid extraction process was 100.2 ± 6.5% for dihydrotestosterone glucuronide and 96.9 ± 9.5% for the internal standard testosterone glucuronide. To study the effect of DHT or *t*-AND on TAM glucuronidation, preliminary experiments were conducted at three concentrations of TAM (1.51, 7.57, and 15.14 μM). Detailed kinetic studies on TAM (1.0–100 μM) glucuronidation were conducted in the presence of six DHT or *t*-AND concentrations (25–250 μM). The incubation conditions were as described previously.

Chromatographic Analysis of Glucuronides. Two methods were developed to quantify *trans*-androsterone glucuronide and dihydrotestosterone glucuronide. To characterize the glucuronidation kinetics of DHT and *t*-AND in the absence of a modifier, *trans*-androsterone glucuronide and dihydrotestosterone glucuronide were quantified by an LC-tandem mass spectrometry method with an Agilent 1100 series capillary LC system coupled with a Thermo Finnigan TSQ quantum triple quadrupole mass spectrometer (Thermo Fisher Scientific). Separation was performed on a Thermo BetaBasic-18 column (150 × 0.5 mm, 3 μm; Thermo Fisher Scientific). The mobile phase consisted of 10 mM ammonium formate (A) and methanol (B) and was delivered at a flow rate of 12 μl/min. A linear gradient elution program, beginning with 50% of mobile phase B and then increasing mobile phase B linearly from 50 to 90% over 1 min and holding at 90% of B for 9 min was used. The column was then reequilibrated at initial conditions for 10 min. Both *trans*-androsterone glucuronide and dihydrotestosterone glucuronide eluted at 7.10 min, and the internal standard testosterone glucuronide eluted at 6.71 min. The mass spectrometer was equipped with an ESI interface operated in negative ion mode. Quantification was accomplished in multiple reaction monitoring mode by monitoring a transition pair of *m/z* 465→287 for *trans*-androsterone glucuronide and dihydrotestosterone glucuronide and 463→285 for the internal standard, testosterone glucuronide. Argon was used as the collision gas. The MS operating conditions were optimized as follows: for transandrosterone glucuronide: spray voltage 4000 V, sheath gas pressure 19 mTorr, auxiliary gas pressure 22 mTorr, capillary temperature 355°C, tube lens offset −95, collision pressure 2.2 mTorr, and collision energy 46 V; and for dihydrotestosterone glucuronide: spray voltage 3200 V, sheath gas pressure 19 mTorr, auxiliary gas pressure 5 mTorr, capillary temperature 355°C, tube lens offset −95, collision pressure 1.9 mTorr, and collision energy 44 V. When coincubated with a modifier, *trans*-androsterone glucuronide and dihydrotestosterone glucuronide were quantified by a LC-MS method with an LC-MS 2010A system (Shimadzu, Columbia, MD). Chromatographic separation was accomplished on a Haisil C8 column (5 μm, 100 × 2.1 mm; Higgins Analytical Inc.). For quantitation of dihydrotestosterone glucuronide, the mobile phase consisted of 0.1% of formic acid in water (A) and acetonitrile (B) delivered at a flow rate of 0.25 ml/min with a linear gradient elution program of 30 to 67.5% of B over 5 min, followed by an isocratic hold at 95% of B for 5 min and a 4-min column reequilibration at the initial conditions. The retention times were 4.23 min for dihydrotestosterone glucuronide and 3.87 min for testosterone glucuronide. For the quantitation of *trans*-androsterone glucuronide, the same mobile phase was used, and a similar gradient elution program was applied: 30 to 60% B over 5 min, followed by an isocratic hold at 95% B for another 5 min and a 4-min column reequilibration at the initial conditions. The retention times for *trans*-androsterone glucuronide and testosterone glucuronide were 3.60 and 3.23, respectively. The mass spectrometer was equipped with an ESI source operated in negative ion mode. Quantitation was accomplished in selected ion monitoring mode by monitoring the respective $[M - H]^-$ ions: *m/z* = 465 for *trans*-androsterone glucuronide and dihydrotestosterone glucuronide and *m/z* = 463 for testosterone glucuronide. The MS parameters were as follows: nebulizing gas flow 1.5 l/min; interface bias −3.50 kV; interface current −9.20 μA; heating block temperature 200°C; focus lens +2.5V; entrance lens 50.0 V; RF gain 5660; RF offset 5210; prerod bias +4.2 V; main rod bias +3.5 V; aperture −20.0 V; conversion dynode +7.0 kV; detector −1.9 kV; curved desolvation line voltage −25.0 kV; Q-array DC −35.0 V; and Q-array RF +150.0V.

Both tamoxifen-*N*-glucuronide and lamotrigine-N_2-glucuronide were quantified by LC-MS methods (LCMS-2010A; Shimadzu). Chromatographic separation was accomplished on a Haisil column (C18 5 μm, 100 × 2.1 mm; Higgins Analytical Inc.). The mobile phase, 0.1% formic acid (A) and 0.1% formic in methanol (B), was delivered at a flow rate of 0.25 ml/min with the following linear gradient elution programs: for lamotrigine-N_2-glucuronide, 5 to 40% B for 5 min, 40 to 80% B for 3 min, an isocratic hold at 95% B for 3 min, and column reequilibration for 4 min (lamotrigine glucuronide eluted at 6.92 min and the internal standard morphine-3-glucuronide eluted at 2.90 min); for tamoxifen-*N*-glucuronide, 5 to 40% B for 5 min, 40 to 90% B for 10 min, an isocratic hold at 95% B for 3 min and, column re-equilibration for 4 min (tamoxifen-*N*-glucuronide eluted at 15.68 min and internal standard lamotrigine glucuronide eluted at 5.96 min). The mass spectrometer was operated in positive ion mode with an ESI interface. Quantification was performed in single ion monitoring mode by monitoring *m/z* = 432 ($[M]^+$) for lamotrigine-N_2-glucuronide, *m/z* = 548 ($[M]^+$) for tamoxifen-*N*-glucuronide, and *m/z* = 462 ($[M + H]^+$) for morphine-3-glucuronide. The MS parameters were set as follows: nebulizing gas flow 1.5 l/min; interface bias +4.50 kV; interface current 11.60 μA; heating block temperature 200°C; focus lens −2.5V; entrance lens −50.0 V; RF gain 5620; RF offset 5060; prerod bias −4.2 V; main rod bias −3.5 V; aperture +20.0 V; conversion dynode −8.0 kV; detector −1.5 kV; curved desolvation line voltage +25.0 kV; Q-array DC +35.0 V; and Q-array RF +150.0 V.

Estimation of Nonspecific Protein Binding. Free fractions of DHT, *t*-AND, TAM, and LTG in incubation were estimated with the Hallifax-Houston model (eq. 1) (Hallifax and Houston, 2006), where *C* is protein concentration in milligrams per milliliter and the logP values of DHT, *t*-AND, TAM, and LTG are 3.428, 3.428, 6.064, and 2.04, respectively, and were calculated with the Molinspiration-Interactive logP calculator (http://www.molinspiration.com/services/logp.html).

$$f_u = \frac{1}{1 + C \cdot 10^{0.072 \cdot \log P^2 + 0.067 \cdot \log P - 1.126}} \quad (1)$$

Data Analysis. Glucuronidation kinetic data for each substrate in the absence of modifiers were analyzed by fitting the Michaelis-Menten equation (eq. 2) or an empirical uncompetitive substrate inhibition equation (eq. 3) to the data with Sigma Plot 9.0 (Systat Software Inc., San Jose, CA) and by nonlinear regression:

$$V_0 = \frac{V_{max} \times [S]}{K_m + [S]} \quad (2)$$

$$V_0 = \frac{V_{max}}{1 + \frac{K_m}{[S]} + \frac{[S]}{K_{si}}} \quad (3)$$

V_{max} and K_m in eq. 2 were defined as the maximum velocity and substrate concentration at which velocity is equal to half of the maximum velocity. V_{max} and K_m in eq. 3 have the same definitions as in eq. 2, and K_{si} is the substrate inhibition constant. The appropriate model was selected by visual inspection of the Eadie-Hofstee plots and comparison of the second-order Akaike information criterion and the residual sum of squares. Kinetic parameters were estimated by nonlinear regression analysis with Sigma Plot 9.0.

Glucuronidation kinetics in the presence of modifiers were analyzed initially by calculating the percent rate of control (in the absence of modifiers). Modifiers that increased or decreased glucuronidation rate by greater than 20% were considered

to exhibit activation or inhibition effects, respectively. One-site competitive (eq. 4), noncompetitive (eq. 5), and mixed inhibition (eq. 6) models were applied to analyze the kinetic data, when only inhibition was observed. V_{max} and K_m in eqs. 4, 5, and 6 have the same definitions as above. K_i is the inhibition constant, and the parameter α reflects changes in the inhibition constant K_i. The appropriate model was selected by visual inspection of the Dixon plots and comparison of the second-order Akaike information criterion.

$$V_0 = \frac{V_{max} \times [S]}{K_m \times \left(1 + \frac{[I]}{K_i}\right) + [S]} \quad (4)$$

$$V_0 = \frac{V_{max} \times [S]}{K_m \times \left(1 + \frac{[I]}{K_i}\right) + [S] \times \left(1 + \frac{[I]}{K_i}\right)} \quad (5)$$

$$V_0 = \frac{V_{max} \times [S]}{K_m \times \left(1 + \frac{[I]}{K_i}\right) + [S] \times \left(1 + \frac{[I]}{\alpha K_i}\right)} \quad (6)$$

Various two-site kinetic models were applied to describe substrate inhibition kinetics as well as the interactions between TAM and DHT or TAM and *t*-AND (Fig. 2; eqs. 7–11). Kinetic models with two-substrate binding sites have been successfully used to explain substrate inhibition kinetics (Houston and Kenworthy, 2000; Lin et al., 2001; Schrag and Wienkers, 2001). The two-site substrate inhibition model, incorporated herein (Fig. 2A; eq. 7), assumes one reaction site and sequential binding of substrate molecules (Galetin et al., 2002). Kinetic models shown in Fig. 2, B (eq. 8) and C (eq. 9), were used to describe the interactions between TAM and DHT. In these models, DHT (assumed to have one binding site in UGT1A4) interacts with the substrate inhibition site of TAM (assumed to have two binding sites in UGT1A4). Two kinetic models (Fig. 2D; eq. 10; Fig. 2E; eq. 11) were used to explain the effect of *t*-AND on TAM glucuronidation. These two models assume that both *t*-AND and TAM have two binding sites in UGT1A4, and they compete for binding to UGT1A4 at both binding sites. In Fig. 2D (eq. 10), the reaction site of *t*-AND overlaps with the reaction site of TAM. In Fig. 2E (eq. 11), the reaction site of the *t*-AND reaction overlaps with the substrate inhibition site of TAM. All of the aforementioned two-site kinetic models assume rapid equilibrium (Segel, 1993). The kinetic parameter V_{max} equates to

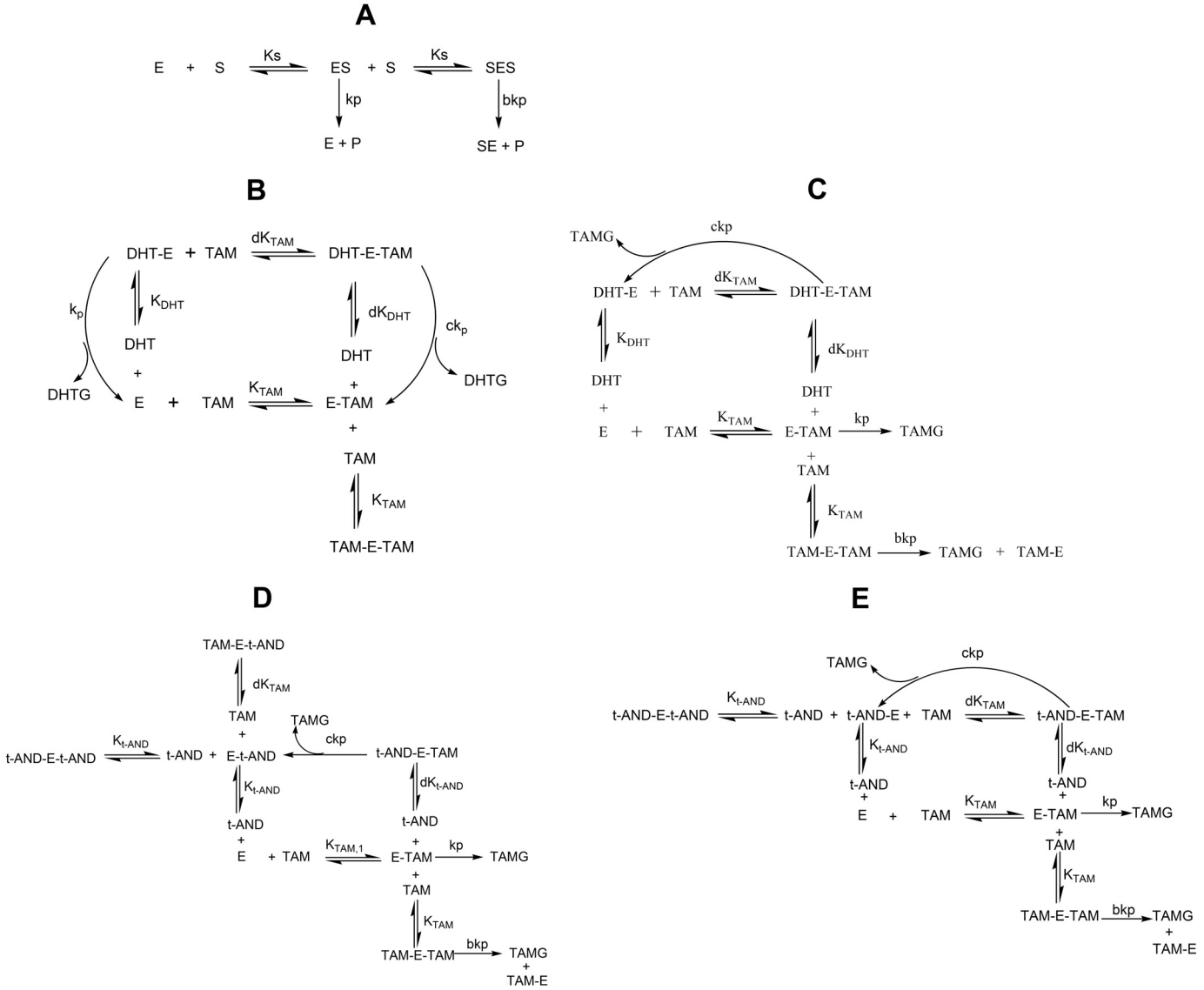

FIG. 2. Two-site kinetic models. A, a kinetic model for substrate inhibition kinetics (eq. 7). B, a kinetic model to explain the effect of TAM on DHT glucuronidation (eq. 8). C, a kinetic model to explain the effect of DHT on TAM glucuronidation (eq. 9). D and E, kinetic models to explain the effect of *t*-AND on TAM glucuronidation (eqs. 10 and 11). k_p is the effective catalytic constant. K_s, K_{DHT}, $K_{t\text{-AND}}$, and K_{TAM} are binding affinity constants. Constant *b* and *c* reflect change in k_p and constant *d* reflects changes in binding affinity. DHTG, DHT glucuronidation; TAMG, TAM glucuronidation.

$k_p[E]_t$, where $[E]_t$ is the total enzyme concentration and k_p is the effective catalytic rate constant. K_s, K_{DHT}, $K_{t\text{-AND}}$, and K_{TAM} are binding affinity constants. Constants b and c reflect changes in k_p. Constant d reflects changes in binding affinity. Surface plots were generated by fitting various two-site models to the kinetic data. Kinetic parameters were estimated with nonlinear regression. Goodness of fit was determined by the residual sum of squares, second-order Akaike information criterion, S.E.s of the parameter estimates and R^2.

$$V_0 = \frac{V_{max} \cdot \left(\frac{[S]}{K_s} + \frac{b \cdot [S]^2}{K_s^2}\right)}{1 + \frac{[S]}{K_s} + \frac{[S]^2}{K_s^2}} \quad (7)$$

$$V_0 = \frac{V_{max} \cdot \left(\frac{[DHT]}{K_{DHT}} + \frac{c \cdot [TAM] \cdot [DHT]}{d \cdot K_{TAM} \cdot K_{DHT}}\right)}{1 + \frac{[DHT]}{K_{DHT}} + \frac{[TAM]}{K_{TAM}} + \frac{[TAM]^2}{K_{TAM}^2} + \frac{[TAM] \cdot [DHT]}{d \cdot K_{TAM} \cdot K_{DHT}}} \quad (8)$$

$$V_0 = \frac{V_{max} \cdot \left(\frac{[TAM]}{K_{TAM}} + \frac{b \cdot [TAM]^2}{K_{TAM}^2} + \frac{c \cdot [TAM] \cdot [DHT]}{d \cdot K_{TAM} \cdot K_{DHT}}\right)}{1 + \frac{[DHT]}{K_{DHT}} + \frac{[TAM]}{K_{TAM}} + \frac{[TAM]^2}{K_{TAM}^2} + \frac{[TAM] \cdot [DHT]}{d \cdot K_{TAM} \cdot K_{DHT}}} \quad (9)$$

$$V_0 = \frac{V_{max} \cdot \left(\frac{[TAM]}{K_{TAM}} + \frac{b \cdot [TAM]^2}{K_{TAM}^2} + \frac{c \cdot [TAM] \cdot [t\text{-AND}]}{d \cdot K_{TAM} \cdot K_{t\text{-AND}}}\right)}{1 + \frac{[t\text{-AND}]}{K_{t\text{-AND}}} + \frac{[t\text{-AND}]^2}{K_{t\text{-AND}}^2} + \frac{[TAM]}{K_{TAM}} + \frac{[TAM]^2}{K_{TAM}^2} + \frac{2 \cdot [TAM] \cdot [DHT]}{d \cdot K_{TAM} \cdot K_{t\text{-AND}}}} \quad (10)$$

$$V_0 = \frac{V_{max} \cdot \left(\frac{[TAM]}{K_{TAM}} + \frac{b \cdot [TAM]^2}{K_{TAM}^2} + \frac{c \cdot [TAM] \cdot [t\text{-AND}]}{d \cdot K_{TAM} \cdot K_{t\text{-AND}}}\right)}{1 + \frac{[t\text{-AND}]}{K_{t\text{-AND}}} + \frac{[t\text{-AND}]^2}{K_{t\text{-AND}}^2} + \frac{[TAM]}{K_{TAM}} + \frac{[TAM]^2}{K_{TAM}^2} + \frac{[TAM] \cdot [DHT]}{d \cdot K_{TAM} \cdot K_{t\text{-AND}}}} \quad (11)$$

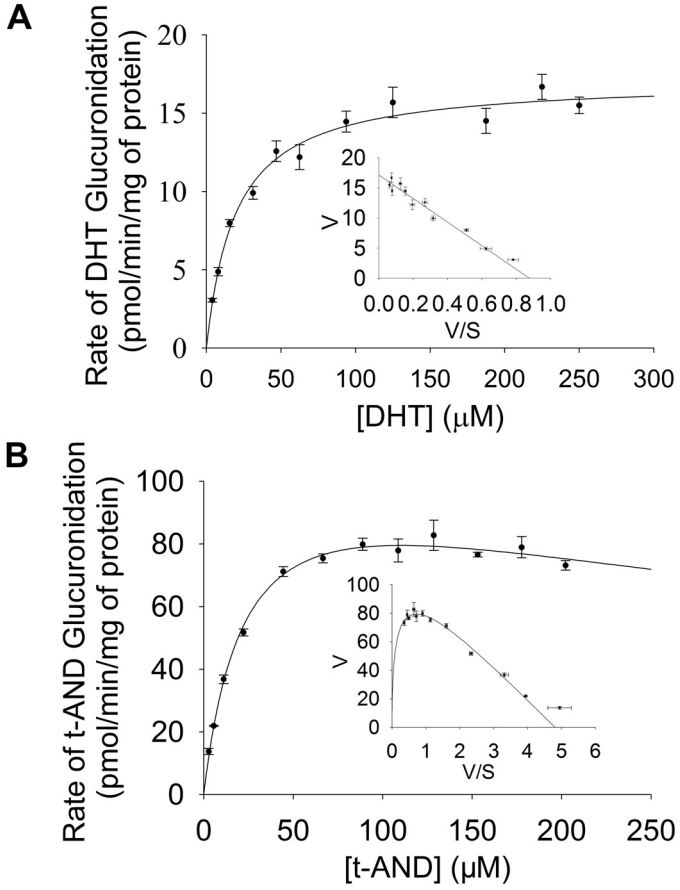

FIG. 3. Kinetic plots (rate versus [S]) for DHT (A) and *t*-AND (B) glucuronidation by recombinant UGT1A4. The bars indicate the range of triplicate measurements. The embedded figures are Eadie-Hofstee plots for the same data. The Michaelis-Menten equation (eq. 2) was fit to the data for DHT glucuronidation. The uncompetitive substrate inhibition equation (eq. 3) was fit to the data for *t*-AND glucuronidation.

Results

Nonspecific Binding of DHT, *t*-AND, TAM, and LTG. The estimated free fractions of DHT and *t*-AND were both 81.2% in incubations with 0.25 mg/ml protein and 91.8% at a protein concentration of 0.1 mg/ml protein. The free fraction of LTG (0.25 mg/ml protein) was estimated to be 95.2%, which is consistent with the negligible binding of LTG to HEK293 cell lysate reported by Rowland et al. (2006). Because the estimated nonspecific binding of DHT, *t*-AND, and LTG under the incubation conditions used was less than 20%, the concentration of DHT, *t*-AND, and LTG added to the incubation mixtures was not corrected for nonspecific protein binding in calculations of kinetic parameters. However, the estimated free fraction of TAM was 11.4% (0.1 mg/ml protein) or 4.5% (0.25 mg/ml protein). TAM concentrations added to the incubation mixtures were corrected for binding when kinetic parameters were estimated.

Kinetics of DHT and *t*-AND Glucuronidation. Initial efforts focused on conducting a detailed evaluation of the kinetics of DHT and *t*-AND glucuronidation. The Michaelis-Menten equation (eq. 2) was fit to the data for DHT glucuronidation, whereas an empirical uncompetitive substrate inhibition equation (eq. 3) was fit to the data for *t*-AND glucuronidation. Results are presented in Fig. 3, and the kinetic parameters obtained by nonlinear regression are presented in Table 1. Although data for *t*-AND glucuronidation were not visually different from fits with the Michaelis-Menten equation in the rate versus [S] plot, fitting the uncompetitive substrate inhibition equation to the data for *t*-AND glucuronidation generated a lower second-order Akaike information criterion (AICc) than fitting the Michaelis-Menten model to the data. [ΔAICc was 19; a value for ΔAICc greater than

TABLE 1

Kinetic parameters for the glucuronidation of DHT, t-AND, TAM, and LTG by recombinant UGT1A4

Data are means (S.E.).

Substrate	K_m	V_{max}	K_{si}	Kinetics Model	R^2
	μM	*pmol/min/mg protein*	*μM*		
DHT	19.6 (2.2)	17.1 (0.44)	N.A.	Michaelis-Menten (eq. 2)	0.9404
t-AND	23.6 (3.1)	114 (7.2)	514 (133)	Uncompetitive substrate inhibition (eq. 3)	0.9755
TAM	0.90 (0.14)	447 (37)	4.6 (0.71)	Uncompetitive substrate inhibition (eq. 3)	0.9639
LTG	1564 (126)	1064 (33)	N.A.	Michaelis-Menten (eq. 2)	0.9926

N.A., not applicable.

10 indicates essentially no support for the unfavorable model (Collom et al., 2008).] In addition, Eadie-Hofstee plots of each data set (Fig. 3) clearly demonstrated differences between the kinetic profiles of DHT and *t*-AND glucuronidation. A two-site substrate inhibition model (Fig. 2A; eq. 7) was also used to describe the data for *t*-AND glucuronidation. The estimated kinetic parameters with this model are presented in Table 2.

Effect of TAM on DHT and *t*-AND Glucuronidation. To test whether differential inhibition can be observed, DHT or *t*-AND was coincubated with a high-affinity UGT1A4 substrate, TAM. TAM, a tertiary amine, forms a quaternary ammonium glucuronide upon UGT1A4-catalyzed *N*-glucuronidation. The reported K_m for TAM glucuronidation with recombinant UGT1A4 is 2.0 ± 0.51 μM (uncorrected for nonspecific binding) (Sun et al., 2006), which was approximately 10-fold lower than the K_m values for glucuronidation on *t*-AND and DHT observed in the present study, suggesting that TAM may serve as a good competitive inhibitor. However, in contrast with the expected competitive inhibition, TAM caused concentration-

TABLE 2

Kinetic parameters obtained by fitting various two-site models to kinetic data

Data are means (S.E.).

Substrate	Modifier	V_{max}	K_{sub}	K_{mod}	*b*	*c*	*d*	Kinetic Model	R^2
		pmol/min/mg protein	*μM*	*μM*					
t-AND	Without modifier	127 (19)	33 (6.0)	N.A.	0.56 (0.12)	N.A.	N.A.	Eq. 7	0.9695
TAM	Without modifier	625 (22)	1.4 (0.12)	N.A.	0.12 (0.02)	N.A.	N.A.	Eq. 7	0.9712
DHT	TAM	9.8 (0.45)	18 (2.2)	0.35 (0.02)	N.A	8.4 (3.0)	4.4 (2.1)	Eq. 8	0.9911
TAM	DHT	562 (43)	1.8 (0.24)	58 (17)	0.10 (0.04)	0.52 (0.20)	2.9 (1.9)	Eq. 9	0.9743
TAM	*t*-AND	761 (51)	1.3 (0.11)	106 (21)	0.18 (0.03)	0.28 (0.12)	1.2 (0.33)	Eq. 10	0.9795
TAM	*t*-AND	761 (51)	1.3 (0.11)	106 (21)	0.18 (0.03)	0.14 (0.06)	0.57 (0.17)	Eq. 11	0.9795

N.A., not applicable. K_{sub}, binding affinity of the substrate; K_{mod}, binding affinity of the modifier.

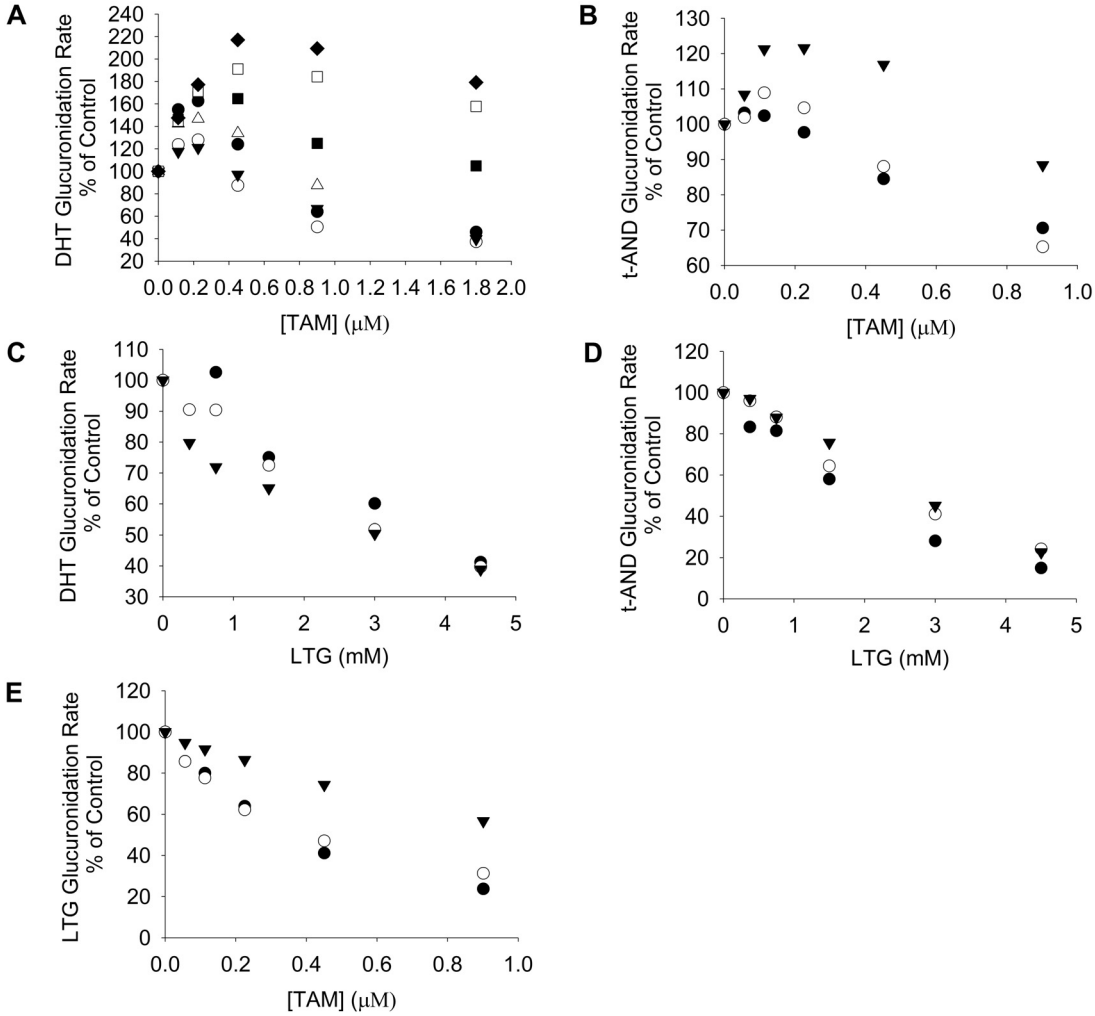

FIG. 4. Rate percentage of control versus [S] plots: for the effect of TAM on DHT glucuronidation (A); for the effect of TAM on *t*-AND glucuronidation (B); for the effect of LTG on DHT glucuronidation (C); for the effect of LTG on *t*-AND glucuronidation (D); and for the effect of TAM on LTG glucuronidation (E). Data points are means of duplicate measurements. Coefficients of variation are all within 10%. Symbols in A represent DHT concentrations: 2.5 (●), 5 (○), 10 (▼), 20 (△), 40 (■), 80 (□), and 100 (◆) μM. Symbols in B, C, and D represent DHT and *t*-AND concentrations: 10 (●), 20 (○), and 40 (▼) μM. Symbols in E represent LTG concentrations: 0.75 (●), 1.5 (○), and 3.0 (▼) mM. TAM concentration in the plots was corrected for nonspecific protein binding. Controls refer to incubations in which the concentration of the modifier was zero.

dependent activation/inhibition of both DHT and *t*-AND glucuronidation (Fig. 4, A and B). For DHT glucuronidation (Fig. 4A), the maximum velocities occurred at concentrations below the highest TAM concentration; i.e., the velocities of DHT glucuronidation initially increased but later decreased as the TAM concentration was increased. In addition, the extent of the activation effect increased as the DHT concentration increased, and the greatest activation was observed at the highest substrate concentration. Statistical comparison of DHT glucuronidation in the presence and absence of 10 μM TAM (uncorrected concentration) at 40 μM DHT indicated that the degree of activation by TAM was statistically significant (Student's *t* test, $P < 0.001$, $n = 6$). With respect to *t*-AND glucuronidation (Fig. 4B), the activation effect of TAM was less pronounced, but features similar to those described above were noted (Fig. 4B). The velocity of *t*-AND glucuronidation initially increased but later decreased with increasing TAM concentration and the extent of activation increased as the *t*-AND concentration was increased.

To better understand the unexpected mixed effects of TAM on DHT glucuronidation, the Michaelis-Menten model (eq. 2) was fit to individual kinetic data sets. The kinetic parameters obtained are shown in Table 3. Both K_m and V_{max} of DHT glucuronidation increased as the TAM concentration was increased. In addition, simultaneous fitting of all kinetic data with a proposed two-site model (Fig. 2B; eq. 8) was conducted and is presented in Fig. 5. Estimated kinetic parameters are presented in Table 2. In the two-site model (Fig. 2B; eq. 8), DHT competes with TAM for binding to the substrate inhibition site of TAM. Models in which DHT competes with TAM for binding to the reaction site of TAM were also used to describe the kinetic data, but much larger S.E.s of the parameter estimates and second-order Akaike information criterion were obtained.

TABLE 3

Kinetic parameters for DHT glucuronidation in the presence or absence of TAM

The Michaelis-Menten equation (eq. 2) was used to fit individual kinetic data sets. Data are means (S.E.). CL_{int} equates to V_{max}/K_m; the TAM concentration was corrected for nonspecific binding.

TAM	K_m	V_{max}	CL_{int}
	μM	*pmol/min/mg protein*	*μl/min/mg protein*
0	17 (1.6)	9.5 (0.3)	0.55
0.11	22 (2.5)	15 (0.60)	0.67
0.23	29 (3.3)	18 (0.79)	0.63
0.45	61 (4.9)	27 (1.1)	0.45
0.90	185 (32)	47 (5.7)	0.25
1.80	227 (89)	47 (14)	0.20

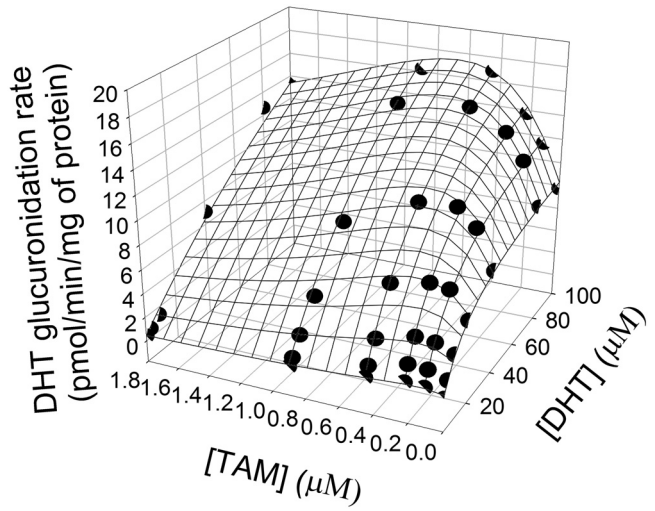

FIG. 5. Kinetic modeling for the effect of TAM on DHT glucuronidation. The surface plot was predicted with eq. 8 (Fig. 2B), and the TAM concentration in the plot was corrected for nonspecific protein binding.

Kinetics of TAM Glucuronidation. Because of the unexpected effect of TAM on DHT and *t*-AND glucuronidation, the kinetics of TAM glucuronidation with recombinant UGT1A4 were evaluated. TAM glucuronidation exhibited substrate inhibition kinetics (Fig. 6). Both the uncompetitive substrate inhibition model (eq. 3) and a two-site model (eq. 7) were fit to the kinetic data. The derived kinetic parameters are presented in Tables 1 and 2, respectively. A constant free fraction of 11.4% for TAM was assumed in calculations of the kinetic parameters.

Effect of LTG on DHT and *t*-AND Glucuronidation. Another amine substrate of UGT1A4, LTG, was also evaluated as a modifier of DHT and *t*-AND glucuronidation. LTG also forms a quaternary ammonium glucuronide upon UGT1A4-catalyzed *N*-glucuronidation. Initially, the kinetics of LTG glucuronidation were evaluated alone. LTG glucuronidation exhibited a hyperbolic kinetic profile (data not shown) with an estimated K_m of 1.6 $\pm$ 0.13 mM (Table 1). LTG at concentrations ranging from $\sim$0.25 K_m to $\sim$3 K_m inhibited DHT and *t*-AND glucuronidation (Fig. 4, C and D). Single-site competitive, noncompetitive, and mixed inhibition models were evaluated to describe the inhibition data. The noncompetitive inhibition model was associated with the lowest AICc values in both cases. The model-predicted lines and observed data are shown in Dixon plots (Fig. 7, A and B). The derived K_i values were 3.25 $\pm$ 0.26 and 2.16 $\pm$ 0.24 mM for DHT and *t*-AND glucuronidation, respectively.

Effects of TAM on LTG Glucuronidation. To investigate whether TAM can activate UGT1A4 with substrates not based on the steroidal ring structure, we also studied the effect of TAM on LTG glucuronidation. At all TAM concentrations tested in the present study, LTG glucuronidation was inhibited (Fig. 4E). A one-site competitive inhibition model was best fit to the inhibition data (Fig. 7C). The K_i for this interaction was 0.31 μM (TAM concentration was corrected for nonspecific protein binding).

Effects of DHT and *t*-AND on TAM Glucuronidation. Finally, the effects of DHT and *t*-AND on TAM glucuronidation were evaluated to assess whether the activation effects were bidirectional. Both *t*-AND and DHT inhibited TAM glucuronidation in a preliminary

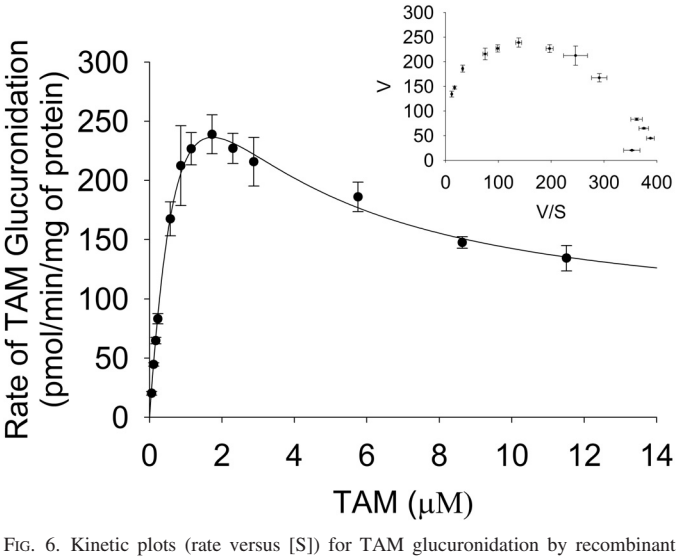

FIG. 6. Kinetic plots (rate versus [S]) for TAM glucuronidation by recombinant UGT1A4. The bars indicate the range of triplicate measurements. The inset shows Eadie-Hofstee plots for the same data. A two-site model (Fig. 2A; eq. 7) was fit to the data.

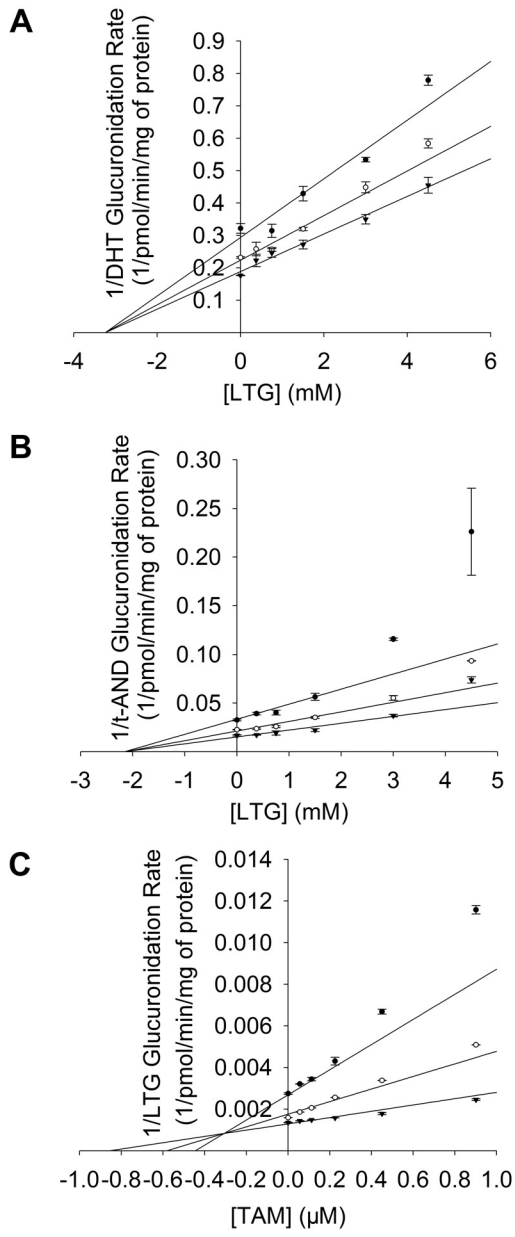

FIG. 7. Dixon plots for inhibition of DHT glucuronidation by LTG (A), for inhibition of *t*-AND glucuronidation by LTG (B), and for inhibition of LTG glucuronidation by TAM (C). The bars indicate the range of duplicate measurements. A one-site noncompetitive inhibition model (eq. 5) was fit to the data in A and B. Symbols represent DHT and *t*-AND concentrations: 10 (●), 20 (○), and 40 (▼) μM. A one-site competitive inhibition model (eq. 4) was fit to the data in C. Symbols represent LTG concentrations: 0.75 (●), 1.5 (○), and 3.0 (▼) mM. The TAM concentration in C was corrected for nonspecific protein binding.

study (data not shown). To gain further insight into the interactions of DHT and *t*-AND on TAM glucuronidation, the kinetics of TAM glucuronidation were evaluated in the presence of six concentrations of DHT or *t*-AND. A two-site substrate inhibition model (eq. 7) was applied to fit the individual kinetic data sets. Although there were no clear trends of changes in the predicted kinetic parameters as DHT or *t*-AND concentration increased, the substrate inhibition kinetic profile of TAM glucuronidation became more hyperbolic (Fig. 8). Various two-site models were tested to simultaneously fit to the kinetic data. The derived kinetic parameters are presented in Table 2. The kinetic model in Fig. 2C (eq. 9) adequately described the effect of DHT on TAM glucuronidation, and the fit of the data are presented in Fig. 8A.

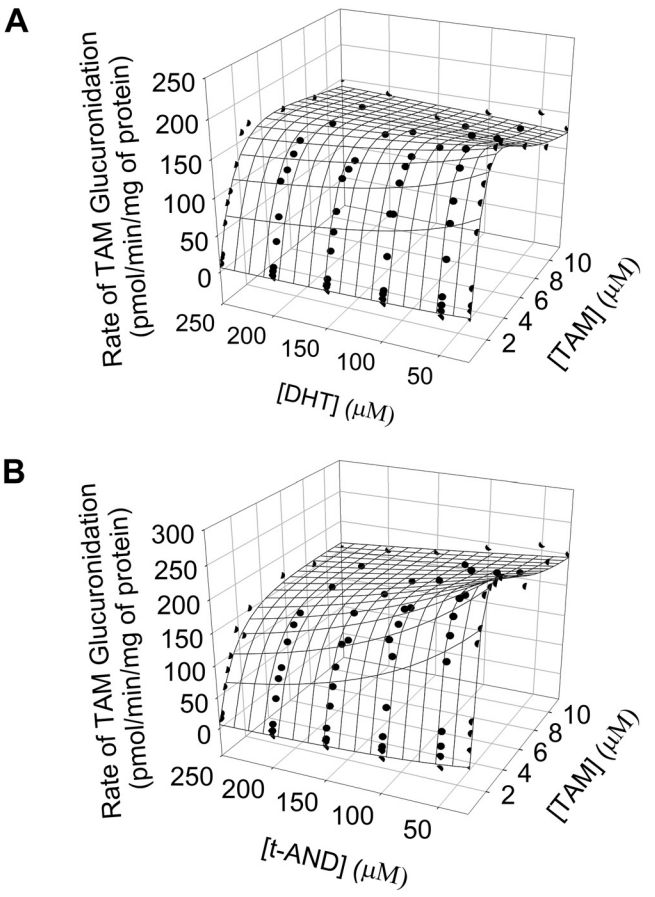

FIG. 8. Kinetic modeling for effect of DHT (A) and *t*-AND (B) on TAM glucuronidation. The surface plot in A is a predicted result with eq. 9 (Fig. 2C), and the surface plot in B is a predicted result with eq. 11 (Fig. 2E). The TAM concentration was corrected for nonspecific protein binding.

For TAM glucuronidation kinetics in the presence of *t*-AND, two kinetic models (Fig. 2D; eq. 10; Fig. 2E; eq. 11) were applied to describe the kinetic data and a similar goodness of fit was obtained. The fit of data to eq. 11 (Fig. 2E) is illustrated in Fig. 8B.

Discussion

In the present study, DHT and *t*-AND (more commonly known as epiandrosterone) were used as probe substrates to evaluate the potential existence of multiple aglycone substrate binding sites in UGT1A4. Glucuronidation of DHT and *t*-AND by HEK293-expressed UGT1A4 was evaluated in the presence of another UGT1A4 substrate, TAM or LTG. Unexpectedly, neither TAM nor LTG competitively inhibited DHT and *t*-AND glucuronidation. Noncompetitive inhibition was observed when LTG was used as the modifier, whereas concentration-dependent activation/ inhibition was observed with TAM as the modifier. These results, combined with kinetic modeling using various two-site models, suggest that multiple substrate binding sites exist in UGT1A4.

The glucuronidation kinetics of the four UGT1A4 substrates under investigation were carefully characterized. DHT and LTG exhibited hyperbolic kinetics, whereas *t*-AND and TAM displayed substrate inhibition kinetics. Although previous studies reported hyperbolic kinetics for TAM glucuronidation by UGT1A4 (Kaku et al., 2004; Sun et al., 2006), there are possible explanations for this discrepancy. In one report, a narrow TAM concentration range (1–6 μM, uncorrected for nonspecific binding) was used, potentially precluding the

observation of substrate inhibition at higher TAM concentrations (Sun et al., 2006). In the second case, a 1-h incubation was conducted (Kaku et al., 2004), suggesting that linear incubation conditions may not have been operational. Our preliminary studies to determine linearity with incubation time and protein concentration for TAM glucuronidation indicated that a low protein concentration and short incubation time were required to maintain steady-state conditions.

In the present study, TAM and *t*-AND substrate inhibition were described with a two-site model, as depicted in Fig. 2A (eq. 7). In both cases, the estimated *b* values were less than 1, indicating that the SES complex is less productive than the ES complex. In addition, consistent with the more pronounced substrate inhibition of TAM glucuronidation, the estimated *b* value for TAM glucuronidation is smaller than the *b* value obtained for *t*-AND glucuronidation.

For UGT-catalyzed glucuronidation, substrate inhibition kinetics can also be explained by the aglycone substrate binding to the enzyme-UDP complex, resulting in a nonproductive dead-end complex (Luukkanen et al., 2005). However, such a mechanism in which only one aglycone substrate binding site is incorporated does not adequately explain the activation effect of TAM on DHT and *t*-AND glucuronidation. UDP, a product of catalysis, has been reported to be an inhibitor for UGT1A4 (IC_{50} = 31 μM) (Fujiwara et al., 2008). It is also possible that the observed substrate inhibition is due to the increased amount of UDP formation at high substrate concentrations. However, the calculated maximum UDP concentration was ~0.5 μM in our study. Thus, the inhibition of UGT1A4 by UDP should be negligible under the incubation conditions used herein.

A few cases of heteroactivation have been reported with UGTs (Williams et al., 2002; Mano et al., 2004; Pfeiffer et al., 2005; Uchaipichat et al., 2008; Hyland et al., 2009). In the present study, TAM both activated and inhibited DHT glucuronidation in a concentration-dependent fashion. A two-site kinetic model (Fig. 2B; eq. 8), which considers the kinetic properties of DHT and TAM, adequately explained the effect of TAM on DHT glucuronidation. In this model, the overall effect of TAM is controlled by three enzyme-associated complexes (E-TAM, TAM-E-TAM, and TAM-E-DHT). Complexes E-TAM and TAM-E-TAM are not productive. The presence of these complexes results in less enzyme available for association with the substrate (DHT), producing an inhibition effect. However, the DHT-E-TAM complex is more productive than the DHT-E complex (c = 8.36). The presence of the DHT-E-TAM complex leads to activation. At low TAM concentrations, the activation resulting from the presence of the DHT-E-TAM complex overcomes the inhibition effect, resulting in an overall activation effect. At high TAM concentrations, the TAM-E-TAM complex becomes the dominant form for TAM associating with the enzyme, resulting in an overall inhibition effect. Also interestingly, in contrast with most previous reports of enzyme heteroactivation, in which the extent of heteroactivation decreases as the substrate concentration increases (Hutzler et al., 2001; Kenworthy et al., 2001; Uchaipichat et al., 2008), DHT glucuronidation is increasingly heteroactivated by TAM as the substrate (DHT) concentration was increased. This discrepancy is probably due to different mechanisms of heteroactivation. In previous cases, heteroactivation was largely due to the positive cooperative binding of substrates and modifiers to the enzyme (Hutzler et al., 2001; Kenworthy et al., 2001; Uchaipichat et al., 2008). However, in the present study, the increased glucuronidation appeared to be due to the presence of a more productive modifier-E-substrate complex (DHT-E-TAM) (c = 8.36). The percentage of the DHT-E-TAM complex among all enzyme complexes is greater at high substrate concentrations than at low substrate concentrations and therefore more activation was observed at high substrate concentrations.

Assuming the same binding scenario as in Fig. 2B (eq. 8), the kinetic model in Fig. 2C (eq. 9) adequately explained the effect of DHT on TAM glucuronidation. But in this case, the predicted c value is less than 1, indicating that the DHT-E-TAM complex is less productive than the E-TAM complex, consistent with the observed inhibition effect of DHT on TAM glucuronidation. In addition, in this model TAM substrate inhibition kinetics would be eliminated as DHT-E-TAM becomes the dominant productive complex, also consistent with our observation that the substrate inhibition kinetic profile of TAM glucuronidation became more hyperbolic as the DHT concentration was increased.

Although the activation is modest, TAM exhibits the same effect on *t*-AND glucuronidation as on DHT glucuronidation: concentration-dependent activation/inhibition and greater activation at higher substrate concentrations. However, the kinetic model in Fig. 2B (eq. 9) may not adequately explain the interactions of TAM on *t*-AND glucuronidation because of the substrate inhibition kinetics of *t*-AND (two *t*-AND binding sites). Kinetic models in which *t*-AND and TAM both have two binding sites on UGT1A4 may be applicable. Kinetic modeling with more data points than obtained in Fig. 4B is needed to adequately characterize the effect of TAM on *t*-AND glucuronidation.

Kinetic studies to characterize the effect of *t*-AND on TAM glucuronidation were carefully conducted. Two kinetic models (Fig. 2D; eq. 10; Fig. 2E; eq. 11) in which the two binding sites of *t*-AND overlap with the two binding sites of TAM adequately explained the kinetic data. Again, the predicted c values (less than 1) are consistent with the inhibition effect of *t*-AND on TAM glucuronidation and TAM substrate inhibition kinetics being eliminated as the less productive *t*-AND-E-TAM complex becomes the dominant productive complex in the models is consistent with our observation.

The unexpected heteroactivation on DHT and *t*-AND glucuronidation by TAM led us to investigate the effect of TAM on UGT1A4 activity with a different type of UGT1A4 substrate: LTG (an aromatic amine substrate of UGT1A4). In contrast to the concentration-dependent activation/inhibition on DHT and *t*-AND glucuronidation, LTG *N*-glucuronidation was competitively inhibited by TAM, suggesting that the heteroactivation of UGT1A4-catalyzed glucuronidation by TAM is substrate-dependent.

LTG was also evaluated as a modifier of DHT and *t*-AND glucuronidation. LTG inhibited both *t*-AND and DHT glucuronidation, but interestingly the one-site noncompetitive inhibition model (eq. 5) better described the kinetic data than the one-site competitive inhibition model (eq. 4). The observed noncompetitive inhibition of DHT glucuronidation by LTG suggests that these two UGT1A4 substrates have distinct binding sites within the active site of UGT1A4, assuming each has only one binding site.

The present study provides compelling evidence for the existence of at least two aglycone binding sites in UGT1A4. Although models can be developed to describe the kinetic data, additional biophysical/biochemical studies are needed to delineate the specific binding region(s) of each molecule in UGT1A4. Additional kinetic studies with a wider range of UGT1A4 substrates are also needed to evaluate the range of substrates for which atypical kinetics are operable. UGT1A4 has been reported to form homodimers (Operana and Tukey, 2007), which may also play a role in these atypical kinetic phenomena. It is yet to be determined whether the two aglycone binding sites exist in different monomers or whether each monomer has two separate aglycone binding sites.

In vitro-in vivo extrapolations for UGT-catalyzed metabolism have proven problematic for a number of reasons, including an inability to estimate in vivo UGT enzyme amounts, lack of isoform-specific probe substrates and inhibitors, overlapping substrate specificities (Miners et

al., 2004, 2006), and the "albumin effect" (Rowland et al., 2008). Accumulating evidence from the current study and others referenced above suggests that atypical kinetics involving this enzyme family may also contribute to the difficulty in making in vitro-in vivo correlations. Atypical kinetic profiles, such as the substrate inhibition observed in the present study, complicate the estimation of intrinsic clearance. In addition, the presence of multiple aglycone binding sites and the substrate-dependent heteroactivation as observed in the present study, complicate the prediction of drug interactions. In summary, the present study reinforces the need for careful characterization of UGT1A4 kinetics and highlights the caveats of making in vitro-in vivo correlations with this important metabolizing enzyme. For the purpose of screening for UGT1A4 inhibitors, the present study suggests the potential need to use multiple probe substrates.

Acknowledgments. We thank Dr. Philip Lazarus at Penn State University for providing transfected HEK-293 cells that express UGT1A4. Synthesis of tamoxifen-*N*-glucuronide was done with the help of Dr. Courtney Aldrich, Center for Drug Design, University of Minnesota. Morphine-3-glucuronide was a gift from Dr. Cheryl Zimmerman, University of Minnesota.

References

Chouinard S, Tessier M, Vernouillet G, Gauthier S, Labrie F, Barbier O, and Bélanger A (2006) Inactivation of the pure antiestrogen fulvestrant and other synthetic estrogen molecules by UDP-glucuronosyltransferase 1A enzymes expressed in breast tissue. *Mol Pharmacol* **69:**908–920.

Collom SL, Laddusaw RM, Burch AM, Kuzmic P, Perry MD Jr, and Miller GP (2008) CYP2E1 substrate inhibition. Mechanistic interpretation through an effector site for monocyclic compounds. *J Biol Chem* **283:**3487–3496.

Fisher MB, Campanale K, Ackermann BL, VandenBranden M, and Wrighton SA (2000) In vitro glucuronidation using human liver microsomes and the pore-forming peptide alamethicin. *Drug Metab Dispos* **28:**560–566.

Fujiwara R, Nakajima M, Yamanaka H, Katoh M, and Yokoi T (2008) Product inhibition of UDP-glucuronosyltransferase (UGT) enzymes by UDP obfuscates the inhibitory effects of UGT substrates. *Drug Metab Dispos* **36:**361–367.

Galetin A, Clarke SE, and Houston JB (2002) Quinidine and haloperidol as modifiers of CYP3A4 activity: multisite kinetic model approach. *Drug Metab Dispos* **30:**1512–1522.

Green MD and Tephly TR (1996) Glucuronidation of amines and hydroxylated xenobiotics and endobiotics catalyzed by expressed human UGT1.4 protein. *Drug Metab Dispos* **24:**356–363.

Hallifax D and Houston JB (2006) Binding of drugs to hepatic microsomes: comment and assessment of current prediction methodology with recommendation for improvement. *Drug Metab Dispos* **34:**724–726; author reply 727.

Hashizume T, Xu Y, Mohutsky MA, Alberts J, Hadden C, Kalhorn TF, Isoherranen N, Shuhart MC, and Thummel KE (2008) Identification of human UDP-glucuronosyltransferases catalyzing hepatic 1α,25-dihydroxyvitamin D3 conjugation. *Biochem Pharmacol* **75:**1240–1250.

Houston JB and Kenworthy KE (2000) In vitro-in vivo scaling of CYP kinetic data not consistent with the classical Michaelis-Menten model. *Drug Metab Dispos* **28:**246–254.

Hutzler JM, Hauer MJ, and Tracy TS (2001) Dapsone activation of CYP2C9-mediated metabolism: evidence for activation of multiple substrates and a two-site model. *Drug Metab Dispos* **29:**1029–1034.

Hyland R, Osborne T, Payne A, Kempshall S, Logan YR, Ezzeddine K, and Jones B (2009) In vitro and in vivo glucuronidation of midazolam in humans. *Br J Clin Pharmacol* **67:**445–454.

Iwuchukwu OF and Nagar S (2008) Resveratrol (*trans*-resveratrol-3,5,4′-trihydroxy-*trans*-stilbene) glucuronidation exhibits atypical enzyme kinetics in various protein sources. *Drug Metab Dispos* **36:**322–330.

Kaku T, Ogura K, Nishiyama T, Ohnuma T, Muro K, and Hiratsuka A (2004) Quaternary ammonium-linked glucuronidation of tamoxifen by human liver microsomes and UDP-glucuronosyltransferase 1A4. *Biochem Pharmacol* **67:**2093–2102.

Kenworthy KE, Clarke SE, Andrews J, and Houston JB (2001) Multisite kinetic models for CYP3A4: simultaneous activation and inhibition of diazepam and testosterone metabolism. *Drug Metab Dispos* **29:**1644–1651.

Kiang TK, Ensom MH, and Chang TK (2005) UDP-glucuronosyltransferases and clinical drug-drug interactions. *Pharmacol Ther* **106:**97–132.

Korzekwa KR, Krishnamachary N, Shou M, Ogai A, Parise RA, Rettie AE, Gonzalez FJ, and Tracy TS (1998) Evaluation of atypical cytochrome P450 kinetics with two-substrate models: evidence that multiple substrates can simultaneously bind to cytochrome P450 active sites. *Biochemistry* **37:**4137–4147.

Lin Y, Lu P, Tang C, Mei Q, Sandig G, Rodrigues AD, Rushmore TH, and Shou M (2001) Substrate inhibition kinetics for cytochrome P450-catalyzed reactions. *Drug Metab Dispos* **29:**368–374.

Luukkanen L, Taskinen J, Kurkela M, Kostiainen R, Hirvonen J, and Finel M (2005) Kinetic characterization of the 1A subfamily of recombinant human UDP-glucuronosyltransferases. *Drug Metab Dispos* **33:**1017–1026.

Mackenzie PI, Rogers A, Treloar J, Jorgensen BR, Miners JO, and Meech R (2008) Identification of UDP glycosyltransferase 3A1 as a UDP N-acetylglucosaminyltransferase. *J Biol Chem* **283:**36205–36210.

Mano Y, Usui T, and Kamimura H (2004) Effects of β-estradiol and propofol on the 4-methylumbelliferone glucuronidation in recombinant human UGT isozymes 1A1, 1A8 and 1A9. *Biopharm Drug Dispos* **25:**339–344.

Miley MJ, Zielinska AK, Keenan JE, Bratton SM, Radominska-Pandya A, and Redinbo MR (2007) Crystal structure of the cofactor-binding domain of the human phase II drug-metabolism enzyme UDP-glucuronosyltransferase 2B7. *J Mol Biol* **369:**498–511.

Miners JO, Knights KM, Houston JB, and Mackenzie PI (2006) In vitro-in vivo correlation for drugs and other compounds eliminated by glucuronidation in humans: pitfalls and promises. *Biochem Pharmacol* **71:**1531–1539.

Miners JO, Smith PA, Sorich MJ, McKinnon RA, and Mackenzie PI (2004) Predicting human drug glucuronidation parameters: application of in vitro and in silico modeling approaches. *Annu Rev Pharmacol Toxicol* **44:**1–25.

Ohno S, Kawana K, and Nakajin S (2008) Contribution of UDP-glucuronosyltransferase 1A1 and 1A8 to morphine-6-glucuronidation and its kinetic properties. *Drug Metab Dispos* **36:**688–694.

Operaña TN and Tukey RH (2007) Oligomerization of the UDP-glucuronosyltransferase 1A proteins: homo- and heterodimerization analysis by fluorescence resonance energy transfer and co-immunoprecipitation. *J Biol Chem* **282:**4821–4829.

Pfeiffer E, Treiling CR, Hoehle SI, and Metzler M (2005) Isoflavones modulate the glucuronidation of estradiol in human liver microsomes. *Carcinogenesis* **26:**2172–2178.

Radominska-Pandya A, Czernik PJ, Little JM, Battaglia E, and Mackenzie PI (1999) Structural and functional studies of UDP-glucuronosyltransferases. *Drug Metab Rev* **31:**817–899.

Rios GR and Tephly TR (2002) Inhibition and active sites of UDP-glucuronosyltransferases 2B7 and 1A1. *Drug Metab Dispos* **30:**1364–1367.

Rowland A, Elliot DJ, Knights KM, Mackenzie PI, and Miners JO (2008) The "albumin effect" and in vitro-in vivo extrapolation: sequestration of long-chain unsaturated fatty acids enhances phenytoin hydroxylation by human liver microsomal and recombinant cytochrome P450 2C9. *Drug Metab Dispos* **36:**870–877.

Rowland A, Elliot DJ, Williams JA, Mackenzie PI, Dickinson RG, and Miners JO (2006) In vitro characterization of lamotrigine N_2-glucuronidation and the lamotrigine-valproic acid interaction. *Drug Metab Dispos* **34:**1055–1062.

Schrag ML and Wienkers LC (2001) Triazolam substrate inhibition: evidence of competition for heme-bound reactive oxygen within the CYP3A4 active site. *Adv Exp Med Biol* **500:**347–350.

Segel I (1993) *Enzyme Kinetics: Behavior and Analysis of Rapid Equilibrium and Steady-State Enzyme Systems.* Wiley Classics Library, Hoboken, NJ.

Shou M, Dai R, Cui D, Korzekwa KR, Baillie TA, and Rushmore TH (2001) A kinetic model for the metabolic interaction of two substrates at the active site of cytochrome P450 3A4. *J Biol Chem* **276:**2256–2262.

Shou M, Grogan J, Mancewicz JA, Krausz KW, Gonzalez FJ, Gelboin HV, and Korzekwa KR (1994) Activation of CYP3A4: evidence for the simultaneous binding of two substrates in a cytochrome P450 active site. *Biochemistry* **33:**6450–6455.

Sun D, Chen G, Dellinger RW, Duncan K, Fang JL, and Lazarus P (2006) Characterization of tamoxifen and 4-hydroxytamoxifen glucuronidation by human UGT1A4 variants. *Breast Cancer Res* **8:**R50.

Tukey RH and Strassburg CP (2000) Human UDP-glucuronosyltransferases: metabolism, expression, and disease. *Annu Rev Pharmacol Toxicol* **40:**581–616.

Uchaipichat V, Galetin A, Houston JB, Mackenzie PI, Williams JA, and Miners JO (2008) Kinetic modeling of the interactions between 4-methylumbelliferone, 1-naphthol, and zidovudine glucuronidation by UDP-glucuronosyltransferase 2B7 (UGT2B7) provides evidence for multiple substrate binding and effector sites. *Mol Pharmacol* **74:**1152–1162.

Uchaipichat V, Mackenzie PI, Guo XH, Gardner-Stephen D, Galetin A, Houston JB, and Miners JO (2004) Human UDP-glucuronosyltransferases: isoform selectivity and kinetics of 4-methylumbelliferone and 1-naphthol glucuronidation, effects of organic solvents, and inhibition by diclofenac and probenecid. *Drug Metab Dispos* **32:**413–423.

Williams JA, Ring BJ, Cantrell VE, Campanale K, Jones DR, Hall SD, and Wrighton SA (2002) Differential modulation of UDP-glucuronosyltransferase 1A1 (UGT1A1)-catalyzed estradiol-3-glucuronidation by the addition of UGT1A1 substrates and other compounds to human liver microsomes. *Drug Metab Dispos* **30:**1266–1273.

Address correspondence to: Dr. Rory P. Remmel, Department of Medicinal Chemistry, College of Pharmacy, University of Minnesota, 308 Harvard St. SE, Minneapolis, MN 55455. E-mail: remme001@umn.edu